PAPER

Check for updates

Analysis of the seasonal water quality variation at the hydraulic junction of a dual-source water distribution system

Bowen Dong,[a] Hui Huang,[a] Chengyan Wang,[a] Xiaolong Zhang,[a] Chenyu Gao,[a] Nan Su,[a] Dayong Shi[a] and Jie Ren [ID] *[b]

The implementation of a dual-source water supply system offers an increased level of reliability in water provision; however, intricate hydraulic dynamics introduce apprehensions regarding water safety at the hydraulic junction. In this study, we gathered data of the water quality at the hydraulic junction of a dual-source water supply system (plant A and plant B, sampling site A_{10} was near plant A, and sampling site A_{12} was near plant B) for one year in Suzhou Industrial Park. Our findings indicated that seasonal variations and water temperature exerted significant influence on the composition and formation of disinfection byproducts (DBPs). Notably, during the warmer months spanning from June to September, the concentration of trihalomethanes was the highest at the hydraulic junction, whereas the concentration of residual chloride was the lowest. The analysis on DBPs revealed that more Br-containing precursors in water in plant A resulted in the accumulation of more Br-containing DBPs at A_{10}, whereas the highest concentration of Cl-containing DBPs accumulated at A_{12}. The analysis of the dissolved organic matter (DOM) composition indicated an increase in concentration at A_{10} and A_{12} compared with that in plant A and plant B. The highest concentration of humic acids was observed at A_{10}, whereas A_{12} accumulated the highest concentration of aromatic proteins and microbial metabolites. Owing to the fluctuations in water consumption patterns at the hydraulic junction, the water quality was susceptible to variability, thereby posing an elevated risk. Consequently, extensive efforts are warranted to ensure the maintenance of water safety and quality at this critical interface.

1. Introduction

Chlorination as a feasible drinking water disinfection technology has been widely promoted.[1,2] However, its associated disinfection byproducts (DBPs) have proven to be toxic to human health. More than 700 species have been observed, which stem from the interactions between chlorine and dissolved organic matters (DOMs).[1,3–6] For example, the U.S. EPA and National Cancer Institute found that trichloromethane (TCM) is carcinogenic towards animals.[7] A 3-decade long observation found that exposure to trihalomethanes (THMs) can cause a decline in the bone density of teenagers.[8] Thus, it is of great importance to understand the formation of DPBs in drinking water distribution systems (DWDSs). Especially in the complex hydraulic section, reciprocation and change in the flow rate, which are derived from the variation in water demand at the end of DWDSs, affect the formation and form of DBPs in DWDSs. Therefore, the investigation of DBPs in DWDSs is beneficial to control the impact of DBPs at the safest level possible.[9–12]

The initial stages of urban development are characterized by the relatively compact populations in cities and towns, leading to the establishment of single-source DWDSs to meet the fundamental water needs of residents. Straightforward hydraulic setups within these pipelines facilitate detailed observations and studies concerning the formation, types, and interplay of DBPs. Peleato *et al.*[13] accurately predicted the species and formation process of DBPs *via* the parallel-factor method. Newhart *et al.*[14] employed artificial neural networks to precisely locate the accumulation and concentration of DBPs in DWDS. However, with the move toward urbanization, the increasing accumulation of population and industry stimulates the demand for clean water, which leads to the incompetence of sole-source DWDS. In this case, extended pipelines, complex DWDS, and even dual-source DWDS are proposed to provide a sufficient water quantity that the sore-source DWDS cannot ensure.[15–17] However, more complex systems also creates greater difficulty in controlling the DBPs given that the hydraulic conditions change a lot. Dong *et al.*[18] highlighted the significant impact of various factors such as different water sources, treatment processes, and enhanced chlorination within the water distribution system (WDS) on the seasonal and spatial variations of disinfection by-product (DBP) distributions during

[a]Gansu Academy of Eco-Environmental Sciences, Lanzhou 730030, China
[b]School of Environment, Harbin Institute of Technology, Harbin, 150090, China

water conveyance. Furthermore, the dual-source DBDS faces a hydraulic mixture of two waters from different water plants, which forms a fluctuated junction at the specific section of the system.[15–17] The overdue hydraulic retention time (HRT) at the valley water consumption period and repeated washouts at the peak water consumption period highlight the complex hydraulic conditions at the conjunction, which makes it more difficult to predict and control DBPs near the junction.[18–22] The interactions between exploited DOMs from the inner wall of the pipelines and the differentiated chemicals at two waters heavily impact the water quality nearby, but scarce investigations have been conducted. Thus, to close the knowledge gap, more efforts should be made to investigate dual-source DWDS, especially in the hydraulic conjunction, which holds significance in ensuring the water quality of cities.[9–12,23]

The current study conducted a comprehensive one-year investigation to monitor the disinfection byproducts (DBPs) within a dual-source drinking water distribution system (DWDS) located in Suzhou Industrial Park. The traditional technique is competent in coping with small-size pipeline networks with high accuracy.[24] Thus, due to the large-size of the network investigated in our work, the employed traditional algorithm was incompetent in accurate prediction, and thus we employed machine learning for further global prediction. We highly acknowledged the contribution of the traditional modelling approach and we will make a further comparison between them and newly developed models in our further work. This system used water from both Lake T and Lake Y as its primary sources. The objectives of this study were threefold, as follows: (1) to examine the influence of spatial and seasonal variations on the formation, types, and interactions of DBPs within the dual-source DWDS; (2) to assess the associated risks and characteristics of DBPs at the hydraulic junction; and (3) to provide practical recommendations for controlling and ensuring the safety of DBPs within DWDS in urban areas.

2. Materials & methods

2.1 Sampling

The dual-source DWDS was located in Suzhou. Water treatment plant A was situated near Lake T and extracted water from this lake at a rate of 0.45 million m^3 per day. The second water treatment plant, plant B, was located near Lake Y and extracted water from this lake at a rate of 0.2 million m^3 per day. The traditional treatment + ozone & activated carbon treatment was used in both plants A and B to purify the original water. The pipelines employed in the DWDS were cast iron pipes. A hydraulic junction was detected at a section 10–12 km away from plant A (Fig. 1). Sampling sites were at the start (A_{10}) and the end (A_{12}) of this hydraulic junction, as well as at the two water treatment plants (A and B). Water samples were collected monthly at each site, with the sampling conducted between 9:00 and 10:00.

Collected water samples were injected with ascorbic acid (dissolved in 0.1 mol L^{-1}) and 1 mol L^{-1} monopotassium phosphate to end the degradation of DBPs and stabilize the
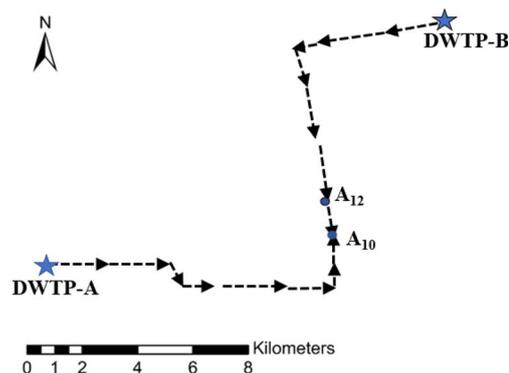

Fig. 1 Dual-source opposite water supply system in this study and sampling sites in this study.

aquatic pH, respectively. Subsequently, the water samples were stored at 4 °C before chemical analysis.

2.2 Analytical methods for common water qualities

The turbidity, aquatic pH, the concentration of algae cell and residual chlorine were detected on the spot using TL2300 (HACH, the USA), PHSJ-3F (Leici, China), YSI-EXOSonde2 (Xylem, Hungary) and DR300 (HACH, the USA), respectively.

2.3 Analytical methods for THMs

A gas chromatography (GC, Agilent 7697A/8890, the USA) equipped with an electrical capture detector (EDC) was employed to quantify the concentration of THMs. The capillary column (HP-5, 30 m × 0.32 mm × 0.25 μm) was initially held at 50 °C for 1 min, then heated to 67.5 °C at a rate of 2.5 °C min^{-1}, and further increased to 120 °C at a rate of 15 °C min^{-1}. The temperatures at the headspace injection and ECD were maintained at 200 °C and 250 °C, respectively. The splitting ratio was fixed at 1 : 50. For headspace sampling, 5 mL of water sample and 15 mL of gas volume were used in sampling bottles. The equilibrium temperature was set at 50 °C and maintained for 60 min.

2.4 Three-dimensional excitation–emission matrix (3D-EEM) analysis

A 3D fluorescence spectrometer (F-7100, Hitachi, Japan) was used to analyze the components of organic matters and the excitation wavelength was 200 : 2 : 400 nm, while the emission wavelength was 250 : 2 : 550 nm. With a scanning speed of 12 000 nm min^{-1} and PTM set at 600 V, each tested sample underwent calibration using the Excitation–Emission Matrix (EEM) of pure water (Milli-Q water) to mitigate the influence of Raman scatter peaks. The obtained EEMs were further analyzed using the fluorescence regional integration (FRI) method with reference to eqn (1), as follows:

$$F_{(i)} = \int_{Ex(i)}^{Ex(j)} \int_{Em(i)}^{Em(j)} I(\lambda_{Ex}\lambda_{Em}) d\lambda_{Ex} d\lambda_{Em} \tag{1}$$

where $F_{(t)}$ is the area integral volume; λ_{Ex} is the corresponding excitation wavelength region; and λ_{Em} is the corresponding emission wavelength region.

2.5 High-performance size-exclusion chromatography (HPSEC) analysis

A gel permeation chromatography (GPC, Prominence, Shimadzu, Japan) equipped with a total organic carbon analyzer (TOC, 1030W, Xylem, Hungary) detector was used to detect the dissolved organic carbon and its molecular weight distribution, while UV_{254} and its molecular weight distribution were detected by an ultraviolet-visible spectrophotometer (UV-VIS, EVO300 PC, Thermo, the USA) detector.

2.6 RDA analysis

CANOCO 5.0 was employed for redundancy analysis (RDA) to analyze the relationship between the indicators and formation of THMs, and Monte Carlo tests were conducted to exclude environmental factors that made small contributions prior to the analysis.

2.7 Raw water analysis of plant-A and plant-B

The turbidity, concentrations of algal cells, UV_{254} and DOC were lower in the source water extracted from Lake Tai than that extracted from Lake Yangcheng. Alternatively, the aquatic pH and bromine ion concentrations were higher in the source water extracted from Lake Yangcheng than that extracted from Lake Tai. Details of the quality of the source water in plant A and B are presented in Table 1.

3. Results and discussion

The water supply of plant A varied with time, while plant B was in a stabilized water supply with ∼7000 m³ h⁻¹. The plateau of water supply was between 8:00 am to 11:00 pm, in which plant A provided over 10 000 m³ h⁻¹ and contributed more than 60% water supply. Hence, plant A acted as the modulator in the water supply system (Fig. 2).

3.1 Temperature significantly mattered in residual chlorine and DBP distribution

Although the two plants applied consistent treatment processes (pre-ozone – coagulation – sedimentation – sand filtration – post-ozone – biological activated carbon filtration – disinfection), there was still some variability in their effluent quality due to the difference of the two water sources. Table 2 shows the variation in several common parameters of water quality at different sampling sites from plant A to plant A. According to Table 2, the change in pH was observed at the water supply distance between A_{10} to A_{12} km, which varied in the range of 7.43–7.82 in the sample sites of plant A and A10 and 7.23–7.59 in the sites of plant B and A12. The turbidity of drinking water is slightly higher in summer and winter (range from 0.10 to 0.17 NTU) than in spring and autumn (range from 0.10 to 0.12 NTU). The variation in UV_{254} showed the same trend as pH at the point of A_{10}-A_{12}, and the UV_{254} value of drinking water served by plant-A was apparently lower than the value served by plant-B. Furthermore, the DOC concentration in the DWDS section near plant B was slightly higher than that near plant A.

Residual chlorine plays a crucial role in the inactivation of pathogens throughout the entire DWDS. In some large-scale

Table 1 Several indexes of raw water quality in plant A and B

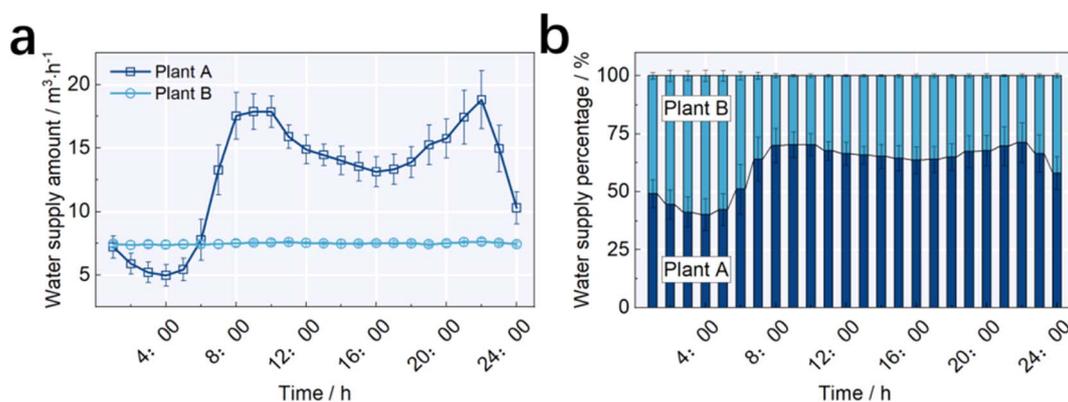| Plant	Turbidity (NTU)	Aqueous pH	Algal cell concentration (million L⁻¹)	UV_{254} (au cm⁻¹)	DOC (mg L⁻¹)	Bromine ion concentration (mg L⁻¹)
A	1.14 ± 0.21	8.40 ± 0.38	0.47 ± 0.58	0.0500 ± 0.0047	3.34 ± 0.27	0.081 ± 0.020
B	14.23 ± 11.80	8.01 ± 0.16	5.73 ± 2.76	0.0661 ± 0.0076	3.77 ± 0.40	0.067 ± 0.013

Fig. 2 Water supply variations over one day. (a) Concrete water supply amount. (b) Contribution of plant A and plant B at different times throughout a day.

Table 2 Several indexes of water sampled in different sites and different seasons

Season	Site	pH	Turbidity (NTU)	UV_{254} (au cm^{-1})	DOC (mg L^{-1})
Spring	Plant A	7.82 ± 0.18	0.10 ± 0.00	0.0257 ± 0.0019	2.56 ± 0.14
	A_{10}	7.74 ± 0.02	0.12 ± 0.04	0.0242 ± 0.0027	2.58 ± 0.09
	A_{12}	7.59 ± 0.01	0.12 ± 0.01	0.0283 ± 0.0056	2.57 ± 0.29
	Plant B	7.57 ± 0.02	0.11 ± 0.01	0.0280 ± 0.0053	2.46 ± 0.34
Summer	Plant A	7.54 ± 0.08	0.15 ± 0.09	0.0243 ± 0.0008	2.45 ± 0.25
	A_{10}	7.47 ± 0.05	0.11 ± 0.02	0.0265 ± 0.0044	2.45 ± 0.23
	A_{12}	7.44 ± 0.15	0.15 ± 0.03	0.0317 ± 0.0018	2.46 ± 0.04
	Plant B	7.36 ± 0.09	0.14 ± 0.01	0.0313 ± 0.0024	2.45 ± 0.06
Autumn	Plant A	7.43 ± 0.09	0.14 ± 0.05	0.0206 ± 0.0018	1.98 ± 0.10
	A_{10}	7.47 ± 0.12	0.11 ± 0.04	0.0213 ± 0.0033	2.03 ± 0.18
	A_{12}	7.29 ± 0.02	0.17 ± 0.02	0.0304 ± 0.0043	2.44 ± 0.18
	Plant B	7.23 ± 0.08	0.14 ± 0.04	0.0323 ± 0.0019	2.51 ± 0.09
Winter	Plant A	7.48 ± 0.03	0.10 ± 0.01	0.0275 ± 0.0029	2.34 ± 0.15
	A_{10}	7.50 ± 0.03	0.10 ± 0.01	0.0168 ± 0.0016	2.33 ± 0.12
	A_{12}	7.31 ± 0.03	0.10 ± 0.01	0.0308 ± 0.0024	2.42 ± 0.42
	Plant B	7.30 ± 0.05	0.11 ± 0.02	0.0329 ± 0.0010	2.55 ± 0.35

supply networks, secondary chlorination may be necessary. However, in this study, no secondary chlorination sites were deployed. According to Fig. 3, the highest residual chlorine was observed at plant A and plant B, with concentrations ranging from 0.7 to 0.9 mg L^{-1}. These values are consistent with the limit of 0.3 mg L^{-1} mandated by the Sanitary Standard for Drinking Water of China. The residual chlorine concentrations at the end of the network (locations A_{10} and A_{12}) ranged from 0.1 to 0.5 mg L^{-1}, which met the minimum requirement of 0.05 mg L^{-1}. The decline in the concentration of residual chlorine alongside the pipelines indicated the consumption of residual chlorine to inactivate pathogens and potential reactions with residual DOMs for the formation of DBPs. The minimum concentration of residual chlorine was observed at A_{10} with an average of 0.31 mg L^{-1} annually. However, a slight increase in the concentration of residual chlorine was observed when the pipelines were extended to A_{12} with an annual record of 0.37 mg L^{-1}. The variation in residual chlorine is a clear indicator of the hydraulic junction, denoting that the junction is between A_{10} to A_{12}. The attenuation of residual chlorine in the distribution system includes 2 categories. One is the main water body attenuation, and the other is the attenuation alongside the pipe wall. The main water body attenuation is caused by the reactions of chlorine with organic matter, inorganic matter and microorganisms in the water body.[9,25–27] The attenuation alongside the pipe wall refers to the attenuation caused by the reactions of chlorine with the sediment, rust and biofilm formed on the pipe wall.[19,20,23] In a single-source DWDS, the concentration of residual chlorine is negatively related to the length of the pipe, and the concentration of residual chlorine is always smaller than the minimum demand at the end of the network. Therefore, secondary chlorination is necessary in this type of distribution system.[21,22,25] On the contrary, the mixture of end water from different sources in a dual-source DWDS avoids secondary chlorination due to the continuous complementary in residual chlorine from two separate sources. The attenuation at the junction is also shaped by the water supply amount.[16,18,27] During the water consumption peak, the frequent domination of water from distinct sources decreased the rate of attenuation. In contrast, the trend was the opposite in the water consumption valley, and the overdue hydraulic retention of water provided enough time for the reaction between residual chlorine and organics in water or biofilm at the inner wall of the pipe.[16,28–31]

3.2 Seasonal influences on species and concentration of DBPs

Clearly, the concentration of residual chlorine was related to the seasonal change. Taking A_{10} for instance, the concentration of
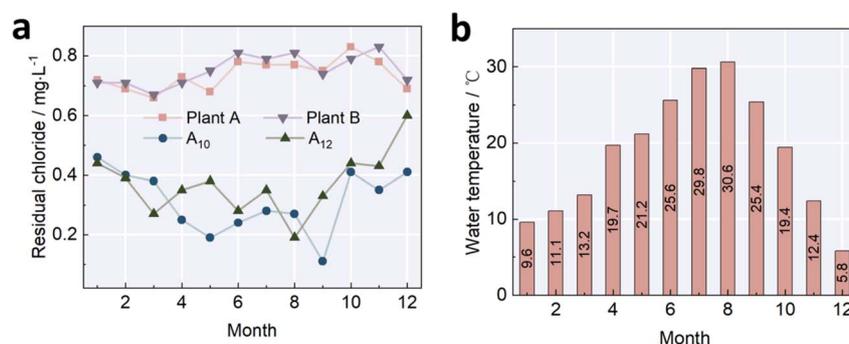

Fig. 3 Concentration of residual chlorine (a) and water temperature (b) at different months.
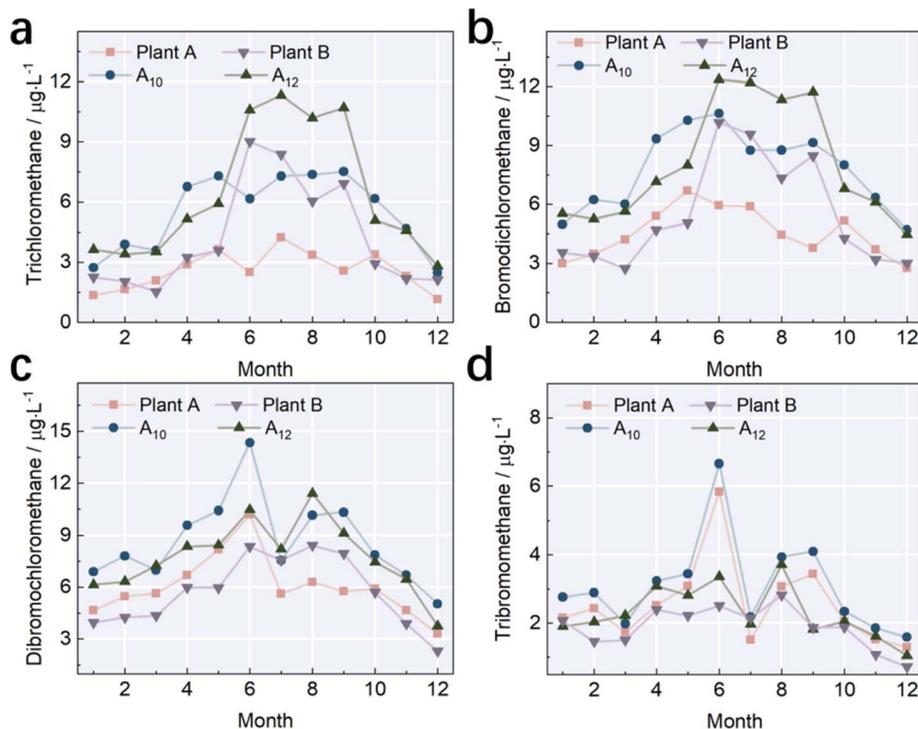
Fig. 4 Concentrations of different DBPs at different months. (a) Trichloromethane (TCM); (b) bromodichloromethane (BDCM); (c) dibromochloromethane (DBCM); and (d) tribromomethane (TBM).

residual chlorine was larger than 0.3 mg L^{-1} from April to September, with aquatic temperatures of 20 °C to 30 °C (Fig. 4). In contrast, the concentration of residual chlorine at A$_{10}$ was smaller than 0.3 mg L^{-1} from October to the next February, with aquatic temperatures of 5 °C to 20 °C. The highest values were at A$_{10}$ in January with an average of 0.46 mg L^{-1} when the aquatic temperature was 9.6 °C (Fig. 3 and 4). This trend is consistent with our analysis of the influence of the temperature on the concentration of DBPs. The relatively low aquatic temperature slowed down the rate of attenuation, pushing the concentration up to a higher level at the hydraulic junction. As the aquatic temperature increased, the acceleration in attenuation caused a decline in the concentration of residual chlorine at the hydraulic junction. Recent reports also found that aquatic temperature showed the biggest influence on the attenuation rate, and the effect of the concentration of organics and the initial concentration of residual chlorine followed the aquatic temperature.[22,29–33]

Furthermore, we detected the species and concentrations of THMs due to their severe toxicity toward human health. As presented in Fig. 4, 4 types of THMs at plant A and plant B were at relatively low concentrations, and then the residual chlorine reacted with THMs alongside the pipelines. Among the 4 THMs, the average concentrations of trichloromethane (TCM) were 2.59 ± 0.95 µg L^{-1}, 5.49 ± 0.91 µg L^{-1}, 6.41 ± 03.29 µg L^{-1} and 4.18 ± 1.26 µg L^{-1} at plant A, A$_{10}$, A$_{12}$ and plant B, respectively. The average concentration of bromodichloromethane (BDCM) was 4.54 ± 1.26 µg L^{-1}, 7.76 ± 2.04 µg L^{-1}, 8.04 ± 3.0 µg L^{-1} and 5.45 ± 2.70 µg L^{-1} at plant A, A$_{10}$, A$_{12}$ and plant B, respectively.

The lower TCM and BDCM concentrations at plant A resulted in lower TCM and BDCM concentrations in the effluent at plant A than that of plant B, with a decline of 38.7% and 23.3%, respectively. Also, the lowest concentration of residual chlorine was observed at A$_{10}$, while the highest TCM and BDCM concentrations were observed at A$_{12}$. The difference in the routine was mainly attributed to the reactions between the residual chlorine and other organics inside the pipelines.[14,20–22]

With the variations in DBP concentration at A$_{10}$ and A$_{12}$ at different months, it was also found that the concentrations of TCM and BDCM were higher at A$_{10}$ in February, March, April, May, October and November. Also, this trend was the opposite in the other months. The concentration of dibromochloromethane (DBCM) was the highest at A$_{10}$ in January, February, April, May, June, September, October, November and December than the other sites, while the concentration of tribromomethane (TBM) was highest at A$_{10}$ throughout the whole year. This observation demonstrated that the minimum concentration of residual chlorine and the maximum DBP concentration was not located at one site but rather settled at different sites with variations in the water supply and water consumption. Temperature played the biggest role in the reactions between residual chlorine and DBPs. The concentrations of THMs were lowest at plant A and plant B in January, February, March, November and December, when the temperature was relatively low during the year. The concentrations of 4 THMs were the highest in June and July, when the water temperature in the pipeline was the highest throughout the year. Wang *et al.*[34] studied the relationships between THMs and pipeline water

temperature in Suzhou also reported similar conclusions. Their study found that the correlation coefficient of THMs and water temperature was positively related to 0.9 and higher. From June to September, the concentrations of THMs were higher than other months at A_{10} and A_{12}, whereas the concentration of residual chlorine was not. This observation suggests that a high water temperature at the junction made it more liable for residual chlorine to react with the precursors of THMs.[20–22,27] The relatively low concentration of residual chlorine could not enable the disinfection effect, and the potential risk was high in this section of the pipeline.

Due to the species of DBPs being diverse in the pipelines, the distributions of the highest concentration of different DBPs were not at the same site. The average concentration of TCM at plant A, plant B, A_{10} and A_{12} was 2.59 ± 0.95 μg L^{-1}, 4.18 ± 2.66 μg L^{-1}, 5.49 ± 1.91 μg L^{-1} and 6.41 ± 3.29 μg L^{-1}, and the concentration of BDCM was 4.54 ± 1.26 μg L^{-1}, 5.45 ± 2.70 μg L^{-1}, 7.76 ± 2.04 μg L^{-1} and 8.04 ± 3.00 μg L^{-1}, respectively. The highest concentrations of TCM and BDCM were observed at A_{12}. The average concentration of TBM at plant A, plant B, A_{10} and A_{12} was 2.55 ± 1.24 μg L^{-1}, 1.82 ± 0.62 μg L^{-1}, 3.08 ± 1.39 μg L^{-1} and 2.30 ± 0.78 μg L^{-1}, and the concentration of DBCM was 6.13 ± 1.77 μg L^{-1}, 5.72 ± 2.02 μg L^{-1}, 8.64 ± 2.46 μg L^{-1} and 7.78 ± 2.05 μg L^{-1}, respectively. The highest concentrations of TBM and DBCM were observed at A_{10}. The concentration of Br^-

was 0.081 mg L^{-1} and 0.067 mg L^{-1} at plant A and plant B, respectively, and thus more precursors of Br^- were at plant A, which can react with residual chlorine. The resultant higher concentrations of DBCM and TBM at plant A than at plant B had values of 6.6% and 28.6% when the 2 plants were applied with the same chlorine addition, respectively. Sun et al.[35] study also proved this opinion. Their study found that the bromine-binding factor (BIF) of TCM increased from 0.5 to 0.8 when the Br^- concentration increased from 100 μg L^{-1} to 300 μg L^{-1}, and the increase in Br^- concentration led to the conversion from chlorinated DBPs to brominated species DBPs.

3.3 Constitution of organics of the water

The residual protein and humic acid may not be removed completely, and thus their detection in water after treatment may occur. Compared with the quantitative analysis by UV_{254} and DOC, the three-dimensional fluorescence spectroscopy method is specialized in both the quantitative and qualitative analysis of organics, which presents high sensitivity and high efficiency without damage to the sample.[6,10,13,21,22,28] We selected samples in July as the target to analyze the constitution of organics in water, and the result is presented in Fig. 5. The regional integral method divided the spectra into 5 pieces, which were located at Ex/Em = (200–250) nm/(260–320) nm (area I), Ex/Em = (200–250) nm/(320–380) nm (area II), Ex/Em =
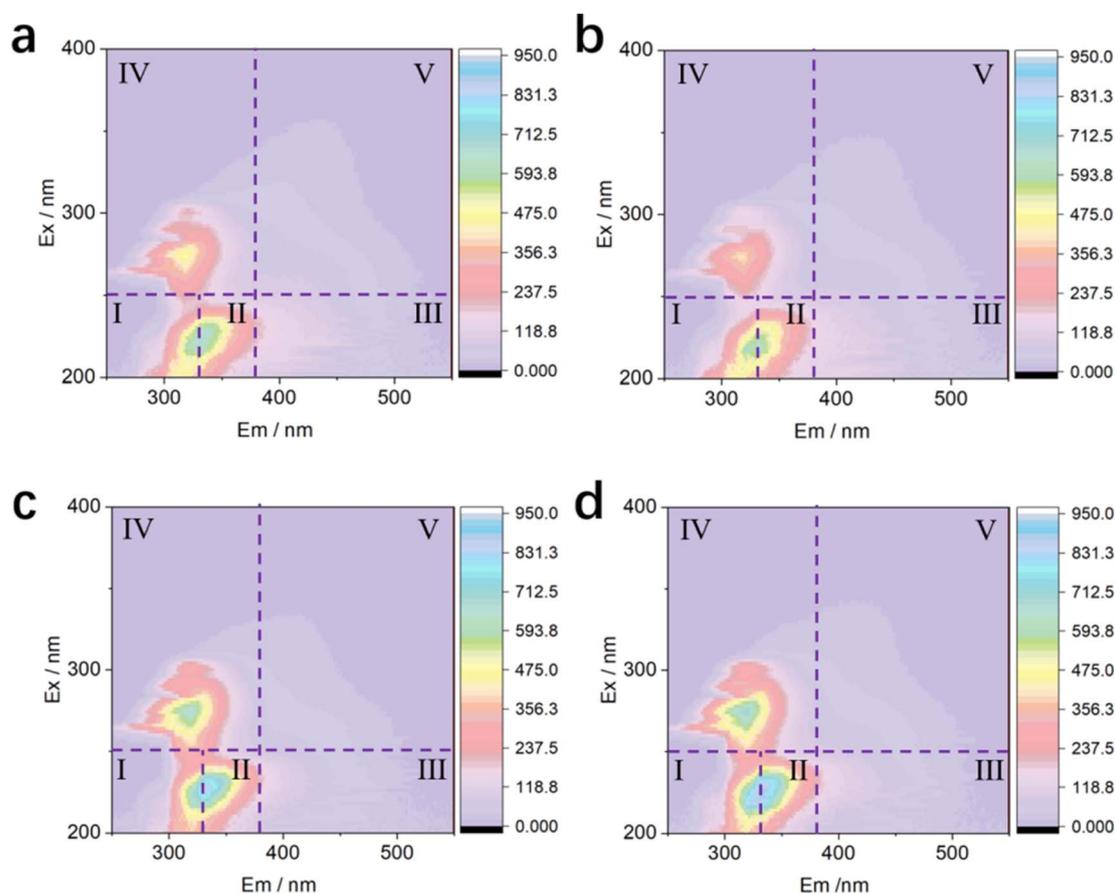

Fig. 5   Three-dimensional fluorescence spectra of different sampling points. (a) Plant A; (b) A_{10}; (c) A_{12}; and (d) plant B.

(200–250) nm/(>380) nm (area III), Ex/Em = (250–450) nm/(260–380) nm (area IV), and Ex/Em = (250–450) nm/(>380) nm (area V), respectively. Area I and II represent the distribution of biodegradable small molecule aromatic proteins. Area III is the distribution of humic acid. Area IV represents the distribution of microbial metabolites such as coenzymes, small organic acids, and pigments. Area V shows the distribution of humic acid with a large molecular weight. The primary distribution of DOM was located at areas I, II and III, and one peak (Fig. 5) was distributed in areas I and II simultaneously, while the other peak was located at area IV. The distribution of 2 peaks represents the existence of tryptophan-like and tyrosine-like substances, which are derived from the metabolism of algae, bacteria and phytoplankton. Some reports also indicated they came from protein-like substances.[10,13,21,22,28]

Fig. 6 shows the variations in the regional integral volume and its values represent the variations in the concentration of organics in an indirect way. As shown in Fig. 6, areas I, II and IV account for a larger part than areas III and V, which is consistent with the aforementioned result that the DOC primarily consisted of aromatic proteins and dissolved microbial metabolites. The regional integral volumes of sample from plant A were 495 100 AU nm^2, 692 160 AU nm^2, 549 510 AU nm^2, 867 330 AU nm^2, and 532 570 AU nm^2, respectively. The integral volumes of the sample from plant B were 542 280 AU nm^2, 833 700 AU nm^2, 416 570 AU nm^2, 1 334 300 AU nm^2, and 389 710 AU nm^2, respectively. The regional integral volumes of samples of plant A in areas I, II and IV were smaller than that of samples of plant B, whereas the regional integral volumes of samples from plant A in area III were larger than that of samples of plant B. These differences denoted that the concentrations of aromatic proteins and microbial metabolites in the samples from plant A were higher than that in the samples from plant B, whereas the concentrations of humic acid showed the opposite trend. The regional integral volumes of the samples had larger values at A_{10} and A_{12} than the samples obtained at plant A and plant B. The highest values in areas I, II, and IV were ascribed to the samples obtained at A_{12}, and the highest values in areas III and V were credited to samples obtained at A_{10}. The observation of

aromatic proteins is usually related to the existence of fluorescent organic waste and dissolved microbial metabolites consisting of colors, proteins, coenzymes and small organic acids.[6,13,28] The high ratio of these organics in water is mainly due to the variations in water quality during its transmission. The main contributors to the variations in the compositions of organics in pipelines are the oxidation by residual chlorine, oxidation by contact between the water and inner wall of the pipeline, and the degradation and metabolism by microbes. The increase in regional integral volume was the largest in area IV as the water was transmitted from plant A or plant B to A_{10} and A_{12}, suggesting that microbial metabolites underwent the largest variation during the water transmission. The second greatest increase in regional integral volume occurred at area II (protein-like chemicals). The biggest variations occurring in areas IV and II were mainly due to the interactions between the oxidants and the shed microbial film, which was liable to form at the inner wall of the cast-iron pipeline. Furthermore, the microbes located at the inner wall produced some proteins, nucleic acids and esters, which can also explain these variations. The main compositions in areas III and IV were humic acid, which is more prone to react with chloride to form precursors of many DBPs. For instance, the interaction between humic acid and chloride generates small aromatic molecules, and then bridges C–Cl bonds *via* chlorination.[10,13,21,22,28] The concentrations of this type of precursor of DBPs depended on the oxidation capability of the disinfectant.

Fig. 7a and c depict the molecular weight distribution of distinct organic matter fractions determined by DOC and UV$_{254}$ detection of the corresponding sample point in July, respectively. The organic matter components in the water were primarily distributed in the range of 0.5 kDa to 10 kDa, with peak positions of DOC and UV$_{254}$ at 2.5 kDa and 8 kDa, respectively. This result was also supported by previous studies.[10] Typically, compounds with molecular weights of >3 kDa were represented by UV$_{254}$.[35] Additionally, the area integration method was utilized to analyze the variations in the different organic matter components based on the molecular weights fractionated into ranges of <1 kDa, 1–3 kDa, 3–10 kDa, and >10 kDa.[10] Changes in the characteristics of organic matter, for example, oxidative degradation of large molecules to small molecules, could be initially detected by the changes in the integrated areas of DOC and UV$_{254}$ in the above ranges.

According to the data presented in Fig. 7b, the integrated area of DOC with molecular weights of < 1 kDa decreased from 0.0051 A.U. at plan A to 0.0037 A.U. at A_{10}, followed by an increase to 0.0060 A.U. at A_{12} and 0.0067 A.U. at plant B. The observed trend was similar to that of residual chlorine, indicating that these substances serve as precursors for THMs. The integrated area of DOC with a molecular weight in the range of 1–3 kDa was recorded as 0.0088, 0.0095, 0.0093, and 0.0142 A.U. at plant A, A_{10}, A_{12}, and plant B, respectively, demonstrating that substances with molecular weights between 1 and 3 kDa at the water supply interface were more liable to be affected by plant A. The integrated area of DOC with a molecular weight between >30 kDa was recorded as 0.0002, 0.0001, 0.0001, and 0.0009 A.U. at plant A, A_{10}, A_{12}, and plant B, respectively. As
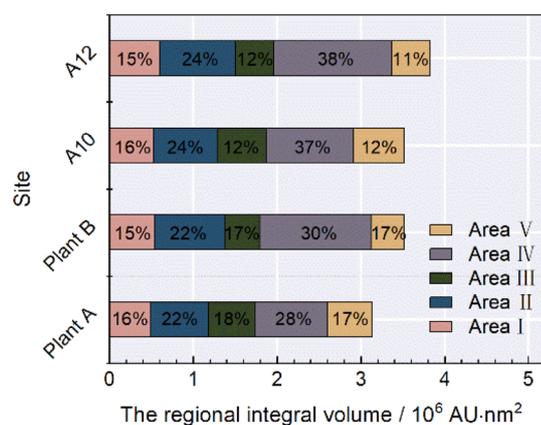

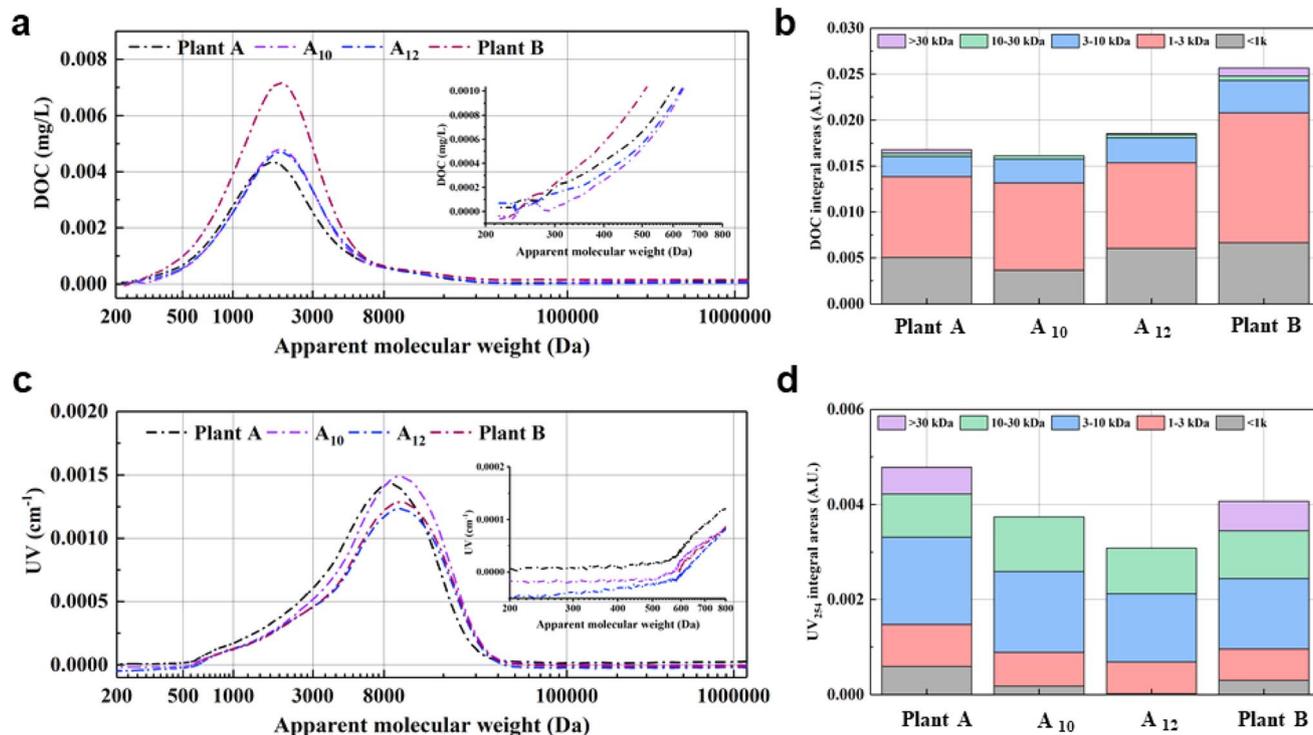Fig. 6 Regional integral volume of three-dimensional fluorescence area at different sampling points.

Fig. 7 HPSEC analysis of organic matters with different molecular weights: (a) molecular weight distribution of DOC; (b) integral areas of DOC; (c) molecular weight distribution of UV_{254} and (d) integral areas of UV_{254}.

shown in Fig. 7d, the integrated area of UV_{254} with molecular weights of <1 kDa decreased from 0.0006 A.U. at plant A to 0.0002 A.U. at A_{10}, followed by an increase from 0.0001 A.U. at A_{12} and 0.0003 A.U. at plant B. Similarly, substances with molecular weights in the range of 3–10 kDa and >30 kDa exhibited a comparable phenomenon. The integrated area at points A_{10} and A_{12} was lower than that of the water from plant A and B. This further suggests that the DOC with higher molecular weights was primarily oxidized and decomposed during the water distribution process.

3.4 Proposed model at the junction of dual-source DWDS

A redundancy analysis (RDA) was conducted to examine the relationship between water quality parameters and THMs, aiming to identify the key factors influencing the formation of THMs. As depicted in Fig. 8, the data accounted for 53.83% and 8.13% of the variance on the first and second axes, respectively. A significant negative correlation ($p < 0.02$) was observed between water temperature (41.6%), residual chlorine (10.1%), and THMs, particularly TBM, based on the RDA analysis. Temperature emerged as a crucial factor affecting residual chlorine decay and THM generation. Secondly, residual chlorine was negatively correlated with the concentration of THMs, which is another important factor affecting the generation of THMs. This result is consistent with previous studies.[36,37] Similarly, DOC (2.0%) and pH (0.3%) were negatively correlated with THMs, but their effects were not as significant as residual chlorine. The impact of water quality parameters on THMs

varied across different sections of the water supply pipeline; for instance, pH, DOC, SUVA, and UV_{254} displayed a negative association with THMs in WDS, whereas turbidity (the explain value only reached 0.1%) exhibited a positive correlation with THMs (Table 3).

The scenario of the hydraulic junction of the dual-source opposite water supply is more complex than DWDS with a single source. A previous study[18,20] suggested that water supply pressures from two DWTPs can counteract each other, leading to stagnation and aging of water in junction pipes. As a result, microorganisms adhering to the pipe walls may release metabolic substances that act as THM precursors. Due to hydraulic
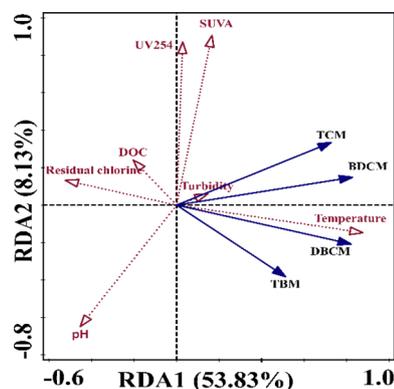

Fig. 8 Redundancy analysis on the relationship between the water quality and different DBPs.

Table 3 The interpretation and results of RDA analysis

Name	Explains (%)	Contribution (%)	Pseudo-F	P
Temperature	41.6	66.5	101.0	0.002
Residual chlorine	10.1	16.1	29.4	0.002
SUVA	8.0	12.8	27.9	0.002
pH	0.3	0.4	1.0	0.380
DOC	2.0	3.2	7.3	0.002
UV_{254}	0.5	0.8	1.8	0.158
Turbidity	0.1	0.2	0.4	0.708

mixing in the junction pipes, the residual chlorine concentration in this area reaches its lowest point, with its location subject to seasonal shifts and influenced significantly by water age. Consequently, optimizing the chlorination dosing process and regularly monitoring THMs within dual-source DWDS are crucial in municipal water management to strike a balance between effective disinfection and THM formation control. We combined the observation in our study and that in the literature and proposed a model of the junction in this study. The complex interactions between the sediment, slime and biofilm formed on the inner wall of the pipeline combined to form irregular rings during the long-term water supply process. In the single-source DWDS, water safety suffered a very limited risk due to the less hydraulic disturbance.[3,15–17,26] However, in the dual-source DWDS, the variation in water consumption was very large and presented a dynamic variation. As water consumption decreased covered by water supply from plant A, the hydraulic junction shifted toward plant B and *vice versa*. This type of variation exacerbated the flourish on the inner wall and enhanced hydraulic mixture and fluctuation. The more unstable hydraulic scenario made it more suitable for biofilm abscission at the inner wall, causing an increase in turbidity and chlorination, and ultimately aggravating the water quality. The hydraulic fluctuation in the hydraulic junction enabled the thorough mixture of residual chlorine and organics, and thus the concentrations of DBPs increased. Furthermore, the hydraulic mixture also allowed the remaining residual chlorine, which avoided the exhaust of residual chlorine occurring in the single-source DWDS. Thus, the disinfection could be ensured. Generally, water quality at the hydraulic junction of dual-source DWDS showed a high risk due to its vulnerability to hydraulic fluctuation, and more efforts should be made to guarantee the water safety and quality in this area.

4 Conclusions

(1) The turbidity was smaller than 0.2 NTU in water both from plant A and plant B. The water pH in plant A was higher than that in plant B, while the concentrations of UV_{254} and DOC showed the opposite trend. The average concentration of organics in A_{10} was higher than that in plant A in Summer and Autumn, while the opposite was observed in Winter and Spring.

(2) Water temperature played the biggest role in the formation and concentration of DBPs and residual chlorine. The concentration of THMs was much higher between June to September than other months at the hydraulic junction. The concentration of residual chlorine was the lowest at A_{10}, while the concentration of TCM and BDCM was the highest at A_{12}. Plant A contained more chlorine-prone brominated precursors, while plant B contained more chlorine-prone chlorine precursors, resulting in higher concentrations of DBCM and TBM at plant A than plant B with values of 6.6% and 28.6% when the 2 plants were applied with the same chloride addition, respectively.

(3) The main composition of DOMs was aromatic protein-like organics and metabolites. The regional integral volume was higher in A_{10} and A_{12} than plant A and plant B. The biggest values were observed at areas I, II and IV at A_{12}, while A_{10} scored the highest values in regional integral volume at areas III and V.

(4) The DOC with higher molecular weights in the range of 3–10 kDa and >30 kDa was primarily oxidized and decomposed during the water distribution process. The substances with molecular weights in the range of 1–3 kDa at the water supply interface could be oxidized and decomposed completely. The hydraulic fluctuation in the hydraulic junction enabled the thorough mixture of residual chlorine and organics, and thus increased the concentrations of DBPs.

Data availability

The datasets obtained during this study are available from the corresponding author upon reasonable request.

Conflicts of interest

The authors declare that they have no known competing financial interests or personal relationships that could have appeared to influence the work reported in this paper.

Acknowledgements

References

1 J. Fu, C. H. Huang, C. Dang and Q. Wang, A review on treatment of disinfection byproduct precursors by biological activated carbon process, *Chin. Chem. Lett.*, 2022, **33**, 4495–4504, DOI: **10.1016/j.cclet.2021.12.044**.

2 X. Yan, T. Lin, X. Wang, S. Zhang and K. Zhou, Effects of pipe materials on the characteristic recognition, disinfection byproduct formation, and toxicity risk of pipe wall biofilms during chlorination in water supply pipelines, *Water Res.*, 2022, **210**, 117980, DOI: **10.1016/j.watres.2021.117980**.

3 K. E. Furst, D. W. Smith, L. R. Bhatta, M. Islam, S. Sultana, M. Rahman, J. Davis and W. A. Mitch, Effects of Intrusion on Disinfection Byproduct Formation in Intermittent Distribution Systems, *ACS ES&T Water*, 2022, **2**, 807–816, DOI: **10.1021/acsestwater.1c00493**.

4 C. G. Li, C. Liu, W.-h. Xu, M. G. Shan and H. X. Wu, Formation mechanisms and supervisory prediction of scaling in water supply pipelines: a review, *Water Res.*, 2022, **222**, 118922, DOI: 10.1016/j.watres.2022.118922.

5 C. Postigo, P. Emiliano, D. Barcelo and F. Valero, Chemical characterization and relative toxicity assessment of disinfection byproduct mixtures in a large drinking water supply network, *J. Hazard. Mater.*, 2018, **359**, 166–173, DOI: 10.1016/j.jhazmat.2018.07.022.

6 X. Xu, B. Wang, J. Shen, J. Kang, S. Zhao, P. Yan and Z. Chen, Characteristics and disinfection by-product formation potential of dissolved organic matter in reservoir water in cold area, *Chemosphere*, 2022, **301**, 134769, DOI: 10.1016/j.chemosphere.2022.134769.

7 X. Sun, M. Chen, D. Wei and Y. Du, Research progress of disinfection and disinfection by-products in China, *J. Environ. Sci.*, 2019, **81**, 52–67, DOI: 10.1016/j.jes.2019.02.003.

8 Y. Sun, Y. X. Wang, C. Liu, V. Mustieles, X. F. Pan, Y. Zhang and C. Messerlian, Exposure to Trihalomethanes and Bone Mineral Density in US Adolescents: A Cross-Sectional Study (NHANES), *Environ. Sci. Technol.*, 2023, **57**, 21616–21626, DOI: 10.1021/acs.est.3c07214.

9 E. N. Bondank, M. V. Chester and B. L. Ruddell, Water Distribution System Failure Risks with Increasing Temperatures, *Environ. Sci. Technol.*, 2018, **52**, 9605–9614, DOI: 10.1021/acs.est.7b01591.

10 Y. Chen, H. Li, W. Pang, B. Zhou, T. Li, J. Zhang and B. Dong, Pilot Study on the Combination of Different Pre-Treatments with Nanofiltration for Efficiently Restraining Membrane Fouling While Providing High-Quality Drinking Water, *Membranes*, 2021, **11**(6), DOI: 10.3390/membranes11060380.

11 H. Huang, B. Dong, N. Wang, Z. Zhang, Y. Wang, J. Ren, H. Li, Z. Xiao and B. Zhou, Revealing Risk Stress on the Lanzhou Section of the Yellow River from the Industries alongside It, *Sustain*, 2022, **14**(22), DOI: 10.3390/su142215235.

12 H. Zhang, Y. Jiang, B. Zhou, Z. Wei, Z. Zhu, L. Han, P. Zhang and Y. Hu, Preparation and photocatalytic performance of silver-modified and nitrogen-doped TiO_2 nanomaterials with oxygen vacancies, *New J. Chem.*, 2021, **45**, 4694–4704, DOI: 10.1039/d0nj04755d.

13 N. M. Peleato, R. L. Legge and R. C. Andrews, Neural networks for dimensionality reduction of fluorescence spectra and prediction of drinking water disinfection by-products, *Water Res.*, 2018, **136**, 84–94, DOI: 10.1016/j.watres.2018.02.052.

14 K. B. Newhart, J. E. Goldman-Torres, D. E. Freedman, K. B. Wisdom, A. S. Hering and T. Y. Cath, Prediction of Peracetic Acid Disinfection Performance for Secondary Municipal Wastewater Treatment Using Artificial Neural Networks, *ACS ES&T Water*, 2021, **1**, 328–338, DOI: 10.1021/acsestwater.0c00095.

15 A. Mohammadi, M. Faraji, A. A. Ebrahimi, S. Nemati, A. Abdolahnejad and M. Miri, Comparing THMs level in old and new water distribution systems; seasonal variation and probabilistic risk assessment, *Ecotoxicol. Environ. Saf.*, 2020, **192**, 110286, DOI: 10.1016/j.ecoenv.2020.110286.

16 S. Potgieter, Z. Dai, M. Havenga, S. Vosloo, M. Sigudu, A. Pinto and S. Venter, Reproducible Microbial Community Dynamics of Two Drinking Water Systems Treating Similar Source Waters, *ACS ES&T Water*, 2021, **1**, 1617–1627, DOI: 10.1021/acsestwater.1c00093.

17 K. Ren, S. Huang, Q. Huang, H. Wang, G. Leng, W. Fang and P. Li, Assessing the reliability, resilience and vulnerability of water supply system under multiple uncertain sources, *J. Cleaner Prod.*, 2020, **252**, 119806, DOI: 10.1016/j.jclepro.2019.119806.

18 F. Dong, Z. Pang, J. Yu, J. Deng, X. Li, X. Ma, A. M. Dietrich and Y. Deng, Spatio-temporal variability of halogenated disinfection by-products in a large-scale two-source water distribution system with enhanced chlorination, *J. Hazard. Mater.*, 2022, **423**, 127113, DOI: 10.1016/j.jhazmat.2021.127113.

19 A. A. Abokifa, Y. J. Yang, C. S. Lo and P. Biswas, Investigating the role of biofilms in trihalomethane formation in water distribution systems with a multicomponent model, *Water Res.*, 2016, **104**, 208–219, DOI: 10.1016/j.watres.2016.08.006.

20 X. Miao, C. Liu, M. Liu, X. Han, L. Zhu and X. Bai, The role of pipe biofilms on dissemination of viral pathogens and virulence factor genes in a full-scale drinking water supply system, *J. Hazard. Mater.*, 2022, **432**, 128694, DOI: 10.1016/j.jhazmat.2022.128694.

21 H. Xu, C. Lin, Z. Shen, L. Gao, T. Lin, H. Tao, W. Chen, J. Luo and C. Lu, Molecular Characteristics of Dissolved Organic Nitrogen and Its Interaction with Microbial Communities in a Prechlorinated Raw Water Distribution System, *Environ. Sci. Technol.*, 2020, **54**, 1484–1492, DOI: 10.1021/acs.est.9b04589.

22 H. Zhou, L. Tian, M. Ni, S. Zhu, R. Zhang, L. Wang, M. Wang and Z. Wang, Effect of dissolved organic matter and its fractions on disinfection by-products formation upon karst surface water, *Chemosphere*, 2022, **308**, 136324, DOI: 10.1016/j.chemosphere.2022.136324.

23 S. M. Premarathna, G. Kastl, I. Fisher and A. Sathasivan, Model for halo-acetic acids formation in bulk water of water supply systems, *Sci. Total Environ.*, 2023, **857**, 159267, DOI: 10.1016/j.scitotenv.2022.159267.

24 M. A. El-khateeb, A. A. E. Galal, M. ElBady and H. I. Abdel-shafy, Chemical properties of drinking water recovered through the application of Pressure Management Activities in Egypt, *Egypt. J. Chem.*, 2023, **66**, 1945–1954, DOI: 10.21608/EJCHEM.2023.220384.8196.

25 L. T. Leonard, G. F. Vanzin, V. A. Garayburu-Caruso, S. S. Lau, C. A. Beutler, A. W. Newman, W. A. Mitch, J. C. Stegen, K. H. Williams and J. O. Sharp, Disinfection byproducts formed during drinking water treatment reveal an export control point for dissolved organic matter in a subalpine headwater stream, *Water Res.*, 2022, **15**, 100144, DOI: 10.1016/j.wroa.2022.100144.

26 T. Maqbool, J. Zhang, Y. Qin, M. B. Asif, Q. V. Ly and Z. Zhang, Fluorescence moieties as a surrogate for residual chlorine in three drinking water networks, *Chem. Eng. J.*, 2021, **411**, 128519, DOI: 10.1016/j.cej.2021.128519.

27 Z. Pang, P. Zhang, X. Chen, F. Dong, J. Deng, C. Li, J. Liu, X. Ma and A. M. Dietrich, Occurrence and modeling of disinfection byproducts in distributed water of a megacity in China: implications for human health, *Sci. Total Environ.*, 2022, **848**, 157674, DOI: **10.1016/j.scitotenv.2022.157674**.

28 C. Fang, X. Yang, S. Ding, X. Luan, R. Xiao, Z. Du, P. Wang, W. An and W. Chu, Characterization of Dissolved Organic Matter and Its Derived Disinfection Byproduct Formation along the Yangtze River, *Environ. Sci. Technol.*, 2021, **55**, 12326–12336, DOI: **10.1021/acs.est.1c02378**.

29 Z. P. Wang and T. Zhang, Characterization of soluble microbial products (SMP) under stressful conditions, *Water Res.*, 2010, **44**, 5499–5509, DOI: **10.1016/j.watres.2010.06.067**.

30 H. Zhang, P. Gao, Y. Liu, Z. Du, L. Feng and L. Zhang, Effects of different types of nitrogen sources in water on the formation potentials of nitrogenous disinfection by-products in chloramine disinfection process based on isotope labeling, *Sci. Total Environ.*, 2022, **842**, 156692, DOI: **10.1016/j.scitotenv.2022.156692**.

31 X. Zhang, J. Shi, X. Huang and B. Shao, Formation and occurrence of disinfection byproducts of benzodiazepine drug estazolam in drinking water of Beijing, *Sci. Total Environ.*, 2022, **804**, 150028, DOI: **10.1016/j.scitotenv.2021.150028**.

32 Z. W. He, W. Z. Liu, C. C. Tang, B. Ling, Z. C. Guo, L. Wang, Y. X. Ren and A. J. Wang, Performance and microbial community responses of anaerobic digestion of waste activated sludge to residual benzalkonium chlorides, *Energy Convers. Manage.*, 2019, **202**, 112211, DOI: **10.1016/j.enconman.2019.112211**.

33 J. Salazar Benitez, C. Mendez Rodriguez and A. Figueroa Casas, Disinfection byproducts (DBPs) in drinking water supply systems: a systematic review, *Phys. Chem. Earth*, 2021, **123**, 102987, DOI: **10.1016/j.pce.2021.102987**.

34 J. Wang, L. Hu, C. Zhao, Y. Su, J. Fu and J. Y. Fu, Primary Investigation on Influencing Factors of Trihalomethanes' Generation in Drinking Water, Water Purification Technology, in Chinese version, *Environ. Sci.*, 2009, **28**, 30–34.

35 X. Sun, J. Liu, X. Zhong, Q. An and S. Sun, Effect of Bromide Ion on Formation Potential of Disinfection By-products in Wastewater Treatment Process, *China Water & Wastewater*, 2022, **38**, 74–80.

36 H. P. Li, R. R. Huo, X. R. Xu, B. Q. Zhou, M. X. Hu, T. Zhou, X. C. Dong, R. Y. Huang, L. Xie and W. H. Pang, Applied gradient boosting decision tree algorithms for accurate prediction of trihalomethanes: a case study in dual-sources drinking water distribution system in metropolitan, *J. Water Process Eng.*, 2023, **56**, 104416, DOI: **10.1016/j.jwpe.2023.104416**.

37 H. P. Li, B. Q. Zhou, X. Y. Xu, R. R. Huo, T. Zhou, X. C. Dong, C. Ye, T. Li, L. Xie and W. H. Pang, The insightful water quality analysis and predictive model establishment via machine learning in dual-source drinking water distribution system, *Environ. Res.*, 2024, **250**, 118474, DOI: **10.1016/j.envres.2024.118474**.